Application Note
JUN 2025
AN-850-0150

Early Spectroscopic Insights into RNA Modifications in LNP Formulations with Microfluidic Modulation Spectroscopy

- ○ Biosimilars
- ○ mAbs
- ○ ADCs
- ○ AAVs
- ○ Ligand Binding
- ○ Protein/Peptide Analysis
- ○ VLPs
- ✓ Nucleic Acid
- ○ Fusion Proteins
- ○ Enzyme Analysis

- ⬢ Aggregation
- ⬢ Quantitiation
- ✓ Structure
- ✓ Stability
- ✓ Similarity

Introduction

Lipid nanoparticles (LNPs) have become the platform of choice for mRNA therapeutics, pairing transcript stabilization with efficient cellular uptake. At their core, ionizable lipids such as SM-102 enable endosomal escape via pH-dependent protonation, but they can also undergo oxidative decomposition to yield electrophilic aldehyde fragments capable of covalently modifying nucleobases. Packer *et al.* first uncovered this phenomenon by isolating a late-eluting mRNA impurity in SM-102-formulated LNPs using reversed-phase ion-pair HPLC.[1] Subsequent LC-MS experiments identified cytidine- and adenine-lipid conjugates, work that has since been backup up by others trying to address this issue with improved ionizable lipid design.[1,2] These adducts likely arise from Schiff-base formation at exocyclic amines or ring nitrogens, as suggested by analogous nucleoside studies.[1,2] Standard workflows couple HPLC-UV of intact RNA with nucleoside profiling by LC-MS, yet these multi-step methods require extensive cleanup and are time-consuming. Further complicating analysis, the mildly acidic ethanolic buffers (pH 5.2) used during LNP assembly accelerate purine depurination and potentially depyrimidation, making it challenging to distinguish covalent adducts from acid-catalyzed abasic site formation.[3] To address these gaps, we have applied UV-Vis spectroscopy and Microfluidic Modulation Spectroscopy (MMS) to homopolymeric adenine and cytosine RNA under formulation-like conditions, enabling direct, label-free monitoring of RNA chemical integrity.

Our UV-Vis and MMS data collected on polyA (purine) and polyC (pyrimidine) samples incubated under LNP-like conditions yield signatures consistent with (1) covalent modification by SM-102-derived aldehydes, (2) acid-catalyzed base cleavage to form abasic sites, or (3) some combination of both mechanisms. PolyA exhibits near-total UV hypochromicity after incubation with SM-102, indicating a loss of aromaticity, while polyC develops a new IR band at 1735 cm^{-1} with attenuated 1655/1604 cm^{-1} peaks, indicating the formation of a new absorbing chemical species. These observations highlight the ability of MMS to detect chemical degradation of RNA with minimal sample workup.

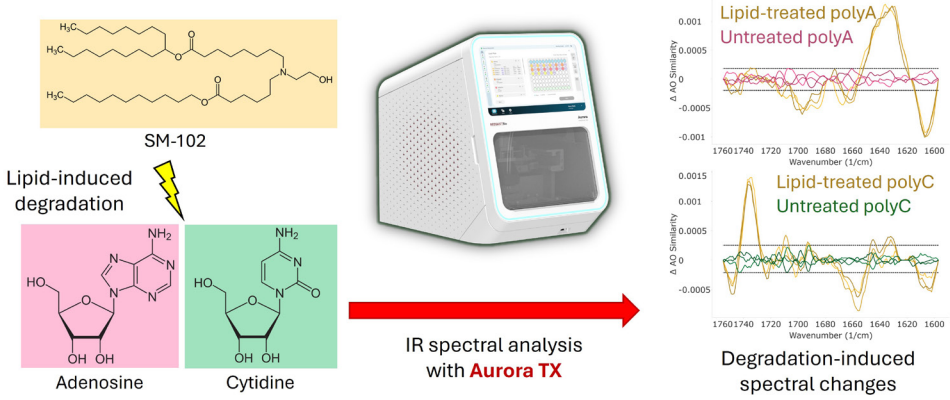

Ionizable lipids like SM-102 are used in the production of lipid nanoparticles to deliver therapeutic RNA. However, these lipids are known to degrade RNA as well. Here, we reproduced experiments in the literature in which polyA and polyC were subjected to conditions similar to those used in the production of LNP mRNA vaccines and demonstrate the ability of MMS to detect spectral changes associated with RNA degradation.

www.redshiftbio.com

REDSHIFTBio®
80 Central Street | Boxborough MA | 01719 | info@redshiftbio.com

Application Note
JUN 2025

Methods

All reagents and buffers were RNase-free. PolyA and polyC (purchased from MilliporeSigma as P9403 and P4903, respectively) were incubated at 0.1 mg/mL for 72 hours at room temperature in 5 mL of 60 mM sodium acetate (pH 5.2), 25% ethanol, and 1 mg/mL SM-102 (Helix Biotech, HLX-0259), as performed by Packer *et al.*[1] Controls omitted SM-102. After incubation, RNA was precipitated with 45 mL isopropanol containing 60 mM ammonium acetate, pelleted at 12,000 × g, rinsed 2 x with 2 mL neat isopropanol, and vacuum-dried overnight. Pellets were resuspended in either neutral buffer (20 mM sodium phosphate, 0.5 mM EDTA, 1 M NaCl, pH 7) or acidic buffer (20 mM ammonium acetate, 0.5 mM EDTA, 1 M NaCl, pH 5.2). UV-Vis spectra (220-350 nm) were recorded on a NanoDrop One (Thermo) in neutral buffer. MMS spectra (1765-1588 cm^{-1}) were acquired on an Aurora TX and analyzed on the RedShift Analytics platform (RedshiftBio). Reference MMS spectra for SM-102 (26% EtOH/PBS), hexanal (PBS), and ribose 5'-phosphate (PBS) were collected.

To prepare SM-102 N-oxide, 0.15 mmol of SM-102 was dissolved in 1.5 mL ethanol and reacted with 0.6 mmol H_2O_2 at 50 °C for 24 hours. After solvent removal under vacuum, the resulting oxidized lipid was used alongside unmodified SM-102 in parallel RNA incubations.[2]

Results

UV–Vis Analysis (Model PolyA and PolyC RNA)

Control polyA shows a strong ~260 nm absorbance (Figure 1). SM-102 treated polyA loses virtually all UV signal, indicating disruption of adenine aromaticity, either by extensive adduct formation or near-complete depurination. Conversely, treated and control polyC spectra overlay exactly, implying intact cytosine aromaticity and suggesting any cytosine modification is confined to its exocyclic amine, which is silent in the UV region.

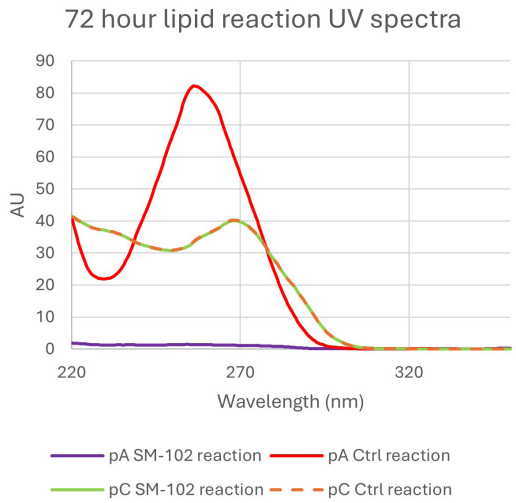

Figure 1: Overlay of UV–Vis spectra for control and SM-102 aldehyde–treated polyA (red vs. purple) and polyC (orange dashed vs. green). Treated polyA shows near-total loss of 260 nm absorbance, while polyC spectra coincide.

MMS Analysis of Model polyA and lipid-treated polyA

At pH 7, treated polyA MMS spectra display slight broadening of the 1654 cm^{-1} peak (NH_2 bend) and a modest decrease at 1606 cm^{-1} (C=C/C=N stretch) versus control (Figure 2A).[4,5] The similarity (Figure 2B) and delta of similarity (Figure 2C) transformations of this data emphasize spectral differences, revealing a shoulder gained between 1642 and 1622 cm^{-1} and loss of intensity at 1654 (NH_2 bend) and 1606 cm^{-1} (C=C/C=N stretch). Meant to aid in spectral comparison, these similarity spectra are baseline-corrected, inverted second derivative plots.

These spectral changes for the polyA sample are not consistent with a simple Schiff base at the exocyclic amine, as suggested in the literature based on mass spectrometry of nucleobases reacted with SM-102.[1,2] Such a reaction would nearly abolish the NH_2 bend[6] and the fitted concentrations of the lipid-treated and control samples are similar by MMS (2.66 mg/mL vs 2.94 mg/mL, respectively), but are consistent with modification at a purine ring nitrogen (e.g., enamine formation), which would disrupt conjugation and UV absorbance. Indeed, even the MMS spectral change is small compared to the change in UV spectra, as the two MMS spectra have roughly 97.12% similarity by area of overlap.

Application Note
JUN 2025

Results, continued

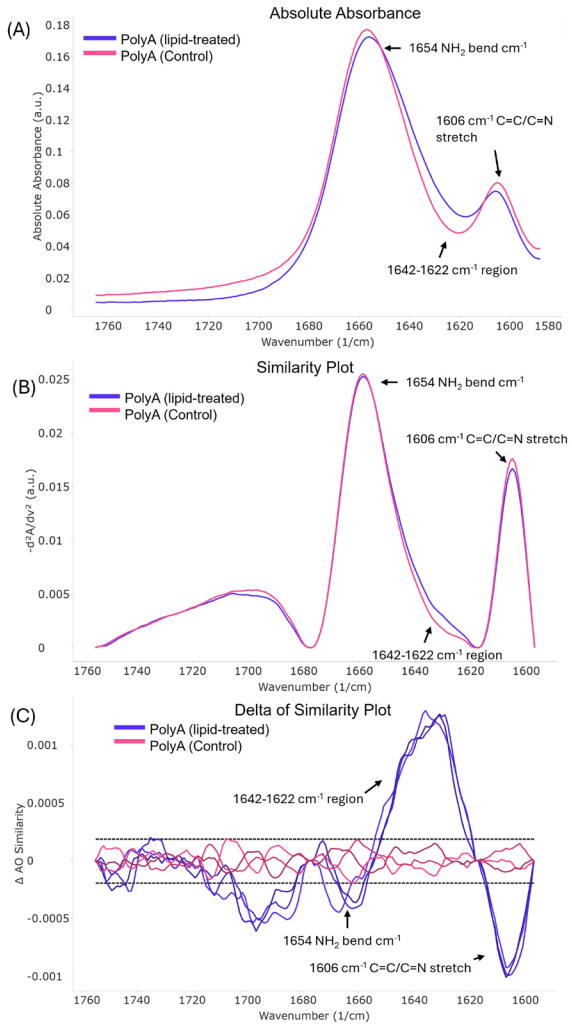

Figure 2. MMS analysis of SM-102-induced degradation of polyA in neutral buffer. (A) Absolute absorbance spectra for control (pink) and SM-102-treated (purple) polyA, displaying broadening of the 1654 cm^{-1} (NH_2) peak and reduced intensity at 1606 cm^{-1} (C=C/C=N). (B) Similarity spectra help to resolve gain of a shoulder between 1642 and 1622 cm^{-1} in the treated sample. (C) The similarity delta plot highlights contrast between the treated and control samples, showing gain in intensity at 1642-1622 cm^{-1} and loss of intensity at 1606 cm^{-1} and 1654 cm^{-1} upon lipid treatment. Spectral similarity is 97.12 % and MMS-derived concentrations are 2.94 mg/mL for control and 2.66 mg/mL for treated.

MMS Analysis of Model polyC and lipid-treated polyC

In neutral buffer, treated polyC exhibits a new band at 1735 cm^{-1} with small losses in signal at 1655 cm^{-1} (C2=O stretch and NH_2 bend) and 1604 cm^{-1} (C=C/C=N stretch) compared to control (Figure 3A).[4,5] The similarity and delta plots (Figure 3B and 3C) accentuate these changes.

Ester functional groups, like those in SM-102 and other lipids, typically absorb near 1750-1735 cm^{-1}. In our SM-102 reference spectrum (Figure 4A and 4B) the ester carbonyl peak (1738 cm^{-1} in 26% EtOH/PBS) does not exactly coincide with the polyC feature, suggesting the 1735 cm^{-1} band may stem from an abasic-site aldehyde (as modeled by ribose 5'-phosphate at 1734 cm^{-1} in PBS). The attenuation at 1655/1604 cm^{-1} further suggests cytosine perturbation, potentially via adduct formation or depyrimidination.

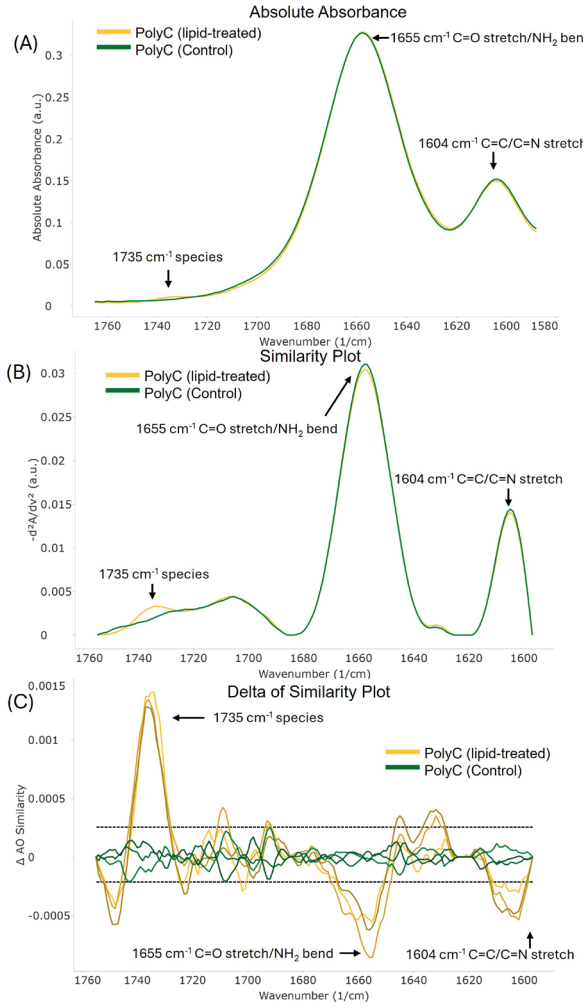

Figure 3. MMS spectral signatures of SM-102 degradation of polyC observed under neutral conditions. (A) Absolute absorbance spectra of untreated polyC (green) and SM-102-treated polyC (yellow) in 20 mM sodium phosphate (pH 7), showing a new 1735 cm^{-1} band and signal loss at 1655 and 1604 cm^{-1}. (B) Similarity spectra and (C) the similarity delta plot highlight the spectral changes shown in (A).

Application Note
JUN 2025

Results, continued

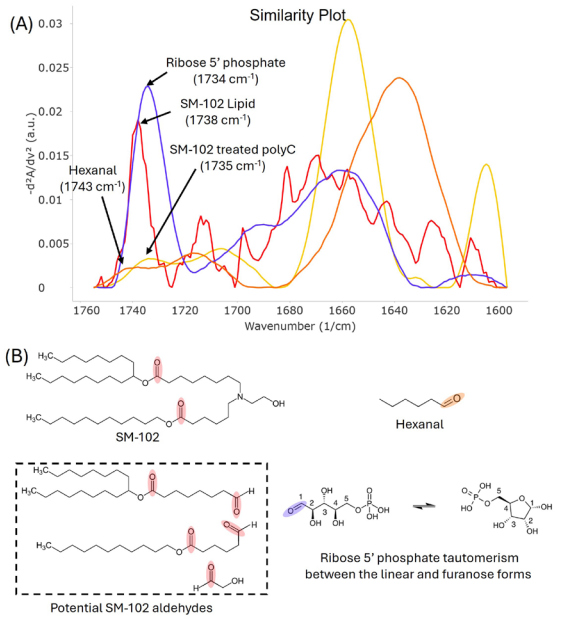

Figure 4. Potential identity of the SM-102-treated PolyC breakdown product. (A) Similarity spectra of treated polyC (yellow), hexanal (orange), SM-102 ester (red), and ribose 5'-phosphate (purple), with ribose 5'-phosphate absorbing at 1734 cm-1. (B) Structures of SM-102, its aldehyde fragments, hexanal, and ribose 5'-phosphate. Spectral similarity between the lipid-treated and untreated polyC was 98.09% and MMS-derived concentrations were ~1.6 mg/mL for both samples.

MMS Analysis of Model polyC i-motif and lipid-treated polyC i-motif

Under acidic conditions, N3 of cytosine is protonated, resulting in the formation of C i-motif secondary structure for cytosine-rich DNA and RNA. This i-motif depends on C-C Hoogsteen base pairing between two parallel strands that are intercalated (i.e. between the bases) of a second pair of parallel, Hoogsteen-base paired strands antiparallel with respect to the first pair (Figure 5A).

In order to assess the effects of SM-102 exposure on base pairing, a pair of lipid-treated and control polyC samples were produced and dissolved into acidic buffer (containing 20 mM ammonium acetate, 0.5 mM EDTA, 1 M NaCl, pH 5.2) instead of the neutral pH buffer to induce i-motif formation. An additional sample treated with a pre-oxidized version of SM-102 (the N-oxide version) was also produced but gave identical results to the sample produced with neat SM-102.

First, the neutral and acidic (i-motif) control samples will be discussed to assign peaks associated with i-motif formation. Compared to the neutral condition, a new peak appears at 1730 cm^{-1} as well as at 1688 cm^{-1} under acidic, i-motif promoting conditions for polyC (Figure 5B and 5C). This is coupled with a dramatic loss of intensity at the 1655 cm^{-1} position corresponding to the unpaired C C2=O stretching and C NH_2 bending modes. Additionally, the peak corresponding to the C=N and C=C stretching modes blue shifts from 1604 cm^{-1} for unpaired cytosine to 1611 cm^{-1} under acidic, i-motif-promoting conditions.

In terms of assignments, the following should be considered provisional. Given the loss of intensity at the 1655 cm^{-1} position corresponding to C C2=O and C NH_2[4,5], the new peaks appearing at 1730 cm^{-1} and 1688 cm^{-1} under i-motif promoting conditions likely correspond to the Hoogsteen base-paired C C2=O and C NH_2, both highly blue shifted. Given that C=O stretches are both typically more intense than NH_2 bends and tend to blue shift to a greater extent than NH_2 bends, the 1730 cm^{-1} peak likely corresponds to the Hoogsteen base paired C C2=O stretch and the 1688 cm^{-1} peak likely corresponds to the Hoogsteen base paired C NH_2 bend. Confirmation would require ^{15}N isotope labeling studies or hydrogen-deuterium exchange, which is beyond the scope of this application note.

Comparing the spectra of the treated and control polyC samples under acidic conditions, there appears to be a small increase in intensity at 1707 cm^{-1} as well as a large dip in intensity at 1655 cm^{-1} that are visible in both the similarity and delta plots (Figure 6). The change in intensity at 1707 cm^{-1} is difficult to interpret since it is a shoulder of a larger peak. However, the loss in intensity at 1655 cm^{-1} may be attributed to changes in the unpaired C NH_2 bending mode, e.g. due to the formation of an adduct at the exocyclic amine or due to limited depyrimidation. Of note, there is a slight increase in intensity under acidic conditions for the peak assigned as the polyC C NH_2 bend for the treated sample (Figure 6), which would be expected to lose intensity upon adduct formation. There was no peak observed at 1735 cm^{-1} under acidic conditions for either sample, which could be attributed to the very intense Hoogsteen-paired C C2=O stretching peak at 1730 cm^{-1} masking it.

Application Note
JUN 2025

Results, continued

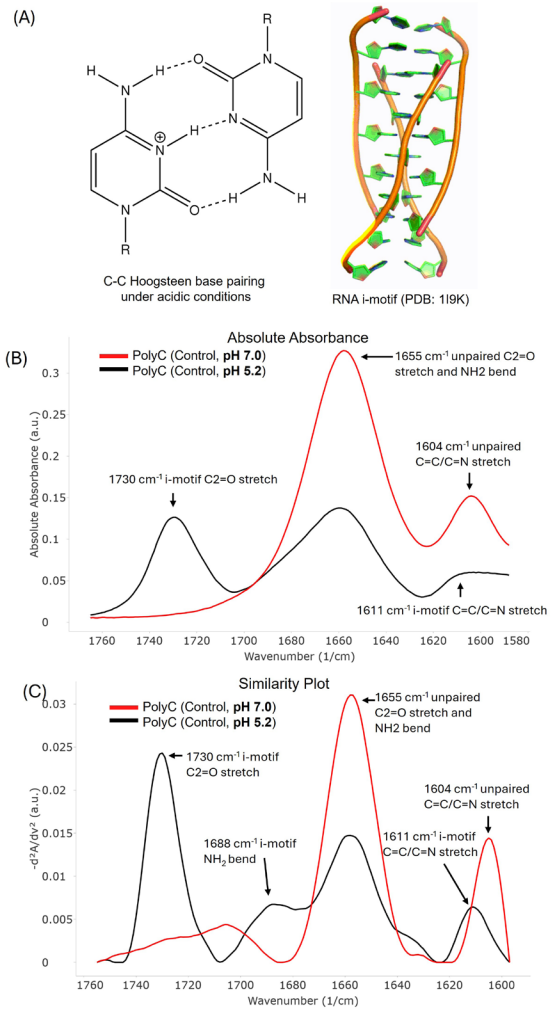

Figure 5. MMS signatures of polyC i-motif formation in acidic buffer. (A) Cytosine-cytosine Hoogsteen pair schematic and i-motif crystal structure (PDB = 1I9K).[7] (B) Absolute absorbance spectra of polyC at pH 5.2 (black) vs. pH 7.0 (red) show the development of a Hoogsteen base-paired C2=O signature at 1730 cm^{-1} and a change in the IR signal of aromatics (shift from 1604 to 1613 cm^{-1}). (C) The similarity plots of (B) reveal an additional peak at 1688 cm^{-1} appearing under acidic, i-motif-promoting conditions provisionally assigned as the Hoogsteen base paired C NH_2. MMS-derived concentrations are 1.6 mg/mL for the polyC control at pH 7.0 and 1 mg/mL for the polyC control at pH 5.2.

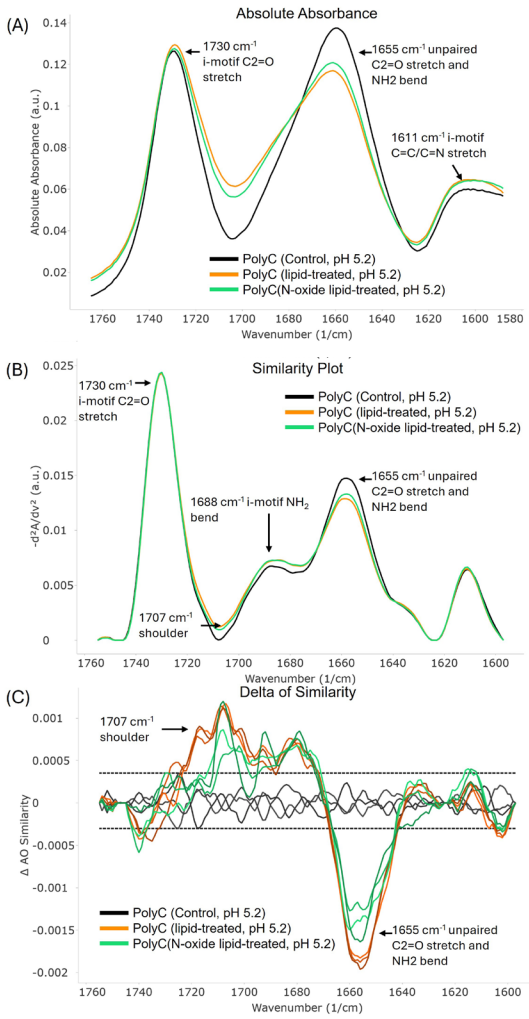

Figure 6. MMS signatures of SM-102 degradation of polyC observed under acidic conditions. (A) Absolute absorbance spectra at pH 5.2 for control (black), SM-102-treated (orange), and N-oxide SM-102-treated (green) polyC. (B) Similarity spectra of (A) showing increases in intensity at the 1707 cm^{-1} shoulder, 1688 cm^{-1} C Hoogsteen paired NH_2 peak, and loss of intensity at the overlapped unpaired C C2=O and NH_2 peak position, which is further highlighted in the delta plot (C). Fitted MMS concentrations are 1 mg/mL for the polyC control, 2.14 mg/mL for the SM-102-treated polyC, and 1.61 mg/mL for the N-oxide SM-102-treated polyC.pH 5.2 at 1.00 mg/mL; SM-102-treated polyC pH 5.2 at 2.14 mg/mL; N-oxide SM-102-treated polyC at pH 5.2 at 1.61 mg/mL; polyC control pH 7.0 at 1.63 mg/mL.

Application Note
JUN 2025

Discussion and Conclusions, continued

Across both UV-Vis and MMS analyses, our data show clear spectral changes in polyA and polyC RNA consistent with several possible degradation mechanisms. In the polyA model, near-total loss of the 260 nm UV absorbance after SM-102 treatment unambiguously indicates severe disruption of adenine's conjugated ring system, either through widespread covalent adduct formation at a ring nitrogen (not the exocyclic amine, since this would not change ring conjugation) or near-complete depurination (Figure 1 and 2). If the primary mechanism is covalent adduct formation, the accompanying MMS spectral changes, such as a subtle shoulder at 1642-1622 cm^{-1} and modest loss at 1606 and 1654 cm^{-1}, support a ring-nitrogen modification (e.g., enamine formation) rather than simple exocyclic amine derivatization. Surprisingly, the MMS spectral perturbations are small (~97% spectral similarity remains) relative to the UV collapse, and the concentrations between the treated and untreated samples are similar by MMS, so we can exclude total acid-catalyzed depurination as causing the loss of UV absorption.

In the polyC model at neutral pH, SM-102 treatment induces a new band at 1735 cm^{-1} alongside attenuated 1655/1604 cm^{-1} peaks (Figure 3). Comparison to reference compounds (hexanal as a lipid aldehyde stand-in, SM-102, and ribose 5'-phosphate as an abasic site stand-in) (Figure 4) shows that ribose 5'-phosphate absorbs closest at 1734 cm^{-1}, suggesting abasic site aldehyde formation, though the other compounds have nearby peaks. The concurrent loss at 1655/1604 cm^{-1} may reflect cytosine exocyclic amine modification or base loss. Notably, pre-oxidation of SM-102 to its N-oxide did not alter these spectral changes, implying that trace aldehyde formation from unoxidized SM-102 is already sufficient to drive modification under these conditions.

Comparing the treated and control polyC samples under acidic i-motif-promoting conditions, the spectral changes seem to indicate a loss of intensity at the 1655 cm^{-1} position corresponding to unpaired C NH_2 and a small increase at 1688 cm^{-1} corresponding to the Hoogsteen paired C NH_2 position (Figure 6). Loss of NH_2 signal is a sign of either depyrimidation or exocyclic amine adduct formation, as secondary amines do not absorb strongly in the Amide I region.[6] Given that the LNP formulation-mimicking reaction conditions also promote C i-motif formation, one possibility is that i-motifs formed and protected parts of the polyC strand from degradation, while the unpaired regions of polyC either were depyrimidated or formed adducts at their exocyclic amines. Exocyclic amine lipid adduct formation for cytosine is a mechanism with some support in the literature.[1,2]

Taken together, these findings are consistent with a model in which SM-102-derived aldehydes may adduct to nucleobase nitrogen atoms and/or possible abasic-site formation, but the relative contributions of each pathway remain unresolved by MMS-based IR measurements alone. To definitively assign covalent structures and quantify base loss, orthogonal techniques will be needed. However, this study has demonstrated the ability of MMS as a quick, first-pass assay to assess degradation in RNA samples that provides the user a direction to follow up on with additional characterization techniques.

Contributor(s)

Scott Gorman, PhD

References

1. Packer M. et al. A novel mechanism for the loss of mRNA activity in lipid nanoparticle delivery systems. *Nat. Commun.* 12, 6777 (2021).

2. Li K. et al. Overcoming thermostability challenges in mRNA–lipid nanoparticle systems with piperidine-based ionizable lipids. *Commun. Biol.* 7, 556 (2024).

3. An R. & Jia Y. Non-enzymatic depurination of nucleic acids: factors and mechanisms. *PLoS ONE* 9, e115950 (2014).

4. Huang, R, Gorman, SD. "Assigning IR Absorption Bands for RNA Building Blocks Using Microfluidic Modulation Spectroscopy." Application Note AN-850-0143. www.redshiftbio.com

5. Gorman, SD, Huang, R. "IR Spectral Signatures of GC, AU, and GU Base Pairing in H2O-based Buffer by Microfluidic Modulation Spectroscopy." Application Note AN-850-0148. www.redshiftbio.com

6. Reusch, W. Infrared Spectroscopy. Virtual Textbook of Organic Chemistry. Michigan State University. Available at: https://www2.chemistry.msu.edu/faculty/reusch/virttxtjml/spectrpy/infrared/irspec1.htm (accessed May 13, 2025).

7. Snoussi, K., Nonin-Lecomte, S. & Leroy, J.-L. The RNA i-motif. *J. Mol. Biol.* 309, 139–153 (2001). https://doi.org/10.1006/jmbi.2001.4618